Beddi Abdelraouf [1], Hicham Serhoud[2], Hebbir Nacer[3]

[1] Institute of Mines, Department of Science Technology, University Larbi Tébessi- Tebessa
[2] Faculty of Technology, Department of Electrical Engineering, University of El-Oued
[3]Faculty of Exact Sciences, Natural, and Life Sciences, Department of Material Sciences, University of Larbi Ben M'hidi, Oum El Bouaghi
ORCID[1]: 0000-0002-5814-3739

doi:10.15199/48.2023.01.21

Comparative study of Sliding Mode and incremental conductance for Maximum Power Point Tracker for Photovoltaic Array

Abstract. *The aim of this paper is to compare two techniques the sliding mode control and incremental conductance, for maximum power point tracking (MPPT) of PV stand-alone system under a rapid change of irradiation and temperature. The comparison study is based on convergence speed, steady-state oscillations, and tracking efficiency. This system consists of a DC/DC boost converter, photovoltaic arrays, load, and MPPT control . The system performance of sliding mode control was compared to the incremental conductance algorithm using the Sim-Power System of MATLAB. From the simulation resulta the sliding mode method shows a better performance and also has a lower oscillation.*

Streszczenie. *Celem tego artykułu jest porównanie dwóch technik, sterowania trybem ślizgowym i przewodności przyrostowej, dla śledzenia punktu maksymalnej mocy (MPPT) w autonomicznym systemie PV przy gwałtownych zmianach napromieniowania i temperatury. Badanie porównawcze opiera się na prędkości zbieżności, oscylacjach stanu ustalonego i wydajności śledzenia. System ten składa się z konwertera doładowania DC/DC, paneli fotowoltaicznych, obciążenia i sterowania MPPT i będzie symulowany przy użyciu systemu Sim-Power firmy MATLAB. Techniki te mają na celu monitorowanie parametrów wyjściowych systemu PV i uzyskanie optymalnego cyklu pracy. Niniejsze opracowanie zawiera szczegółową analizę i porównanie różnych technik. (**Badanie porównawcze trybu przesuwania i przewodnictwa przyrostowego dla modułu śledzenia punktu maksymalnej mocy dla macierzy fotowoltaicznej**)*

Keywords: stand-alone, Converter, MPPT, sliding mode, *incremental conductance*.
Słowa kluczowe: samodzielny, konwerter, MPPT, tryb przesuwny, przewodność przyrostowa.

Introduction

In recent years, the spread of renewable energy resources worldwide are becoming very extensive, which allow people exploiting energy solar to meet their needs on one side and protect the environment on the other side [1]. Conversion efficiency reach of PV arrays from 13 % to 47%, that's not sufficient to meet the needs of consumers[2]. Hence, they increase the number of PV arrays, that affects negatively cost. It becomes necessary to extract as much power as possible from PV arrays, with considering efficacy, cost, and reliability.

This paper presents a comparative study of a DC/DC converter controller in different input information. Many researchers have done for MPPT algorithms, utilizing different control techniques (classic and modern), namely, Perturb and Observe (P&O) [3], incremental conductance [4], hill-climbing[5], Grey wolf optimization [6], genetic algorithm [7], neural networks (ANN) [8], particle swarm optimization (PSO)[9][10], fuzzy logic (FL) [11], predictive control [12], sliding mode (SM) [13], etc. In this current document, we analyze the simulation of photovoltaic system a stand-alone.

The objective of this work is tracking MPP and optimisation the duty cycle of proposed SMC controller ,and the comparison study is for ensure the performance of SMC control.

The description of the comparative study is as follows: Description of system is explained in Section 2. In Section 3, describes the important of MPPT techniques. Section 4, describes comparison and analyses the simulation of respective techniques. The conclusion will be provided in Section 5.

DDescription of a stand-alone system

The term "stand-alone PV system" is used to describe a PV system that is not connected to the grid. A PV panel, DC/DC boost converter, load, and a control circuit MPPT are used to operate the system [8][9]. As show in Figure.1:

The description of study PV systeme parameters:

The modules are connected to PV arrays (2 series and 3 parallel). The specifications of the PV module are as detailed belo:

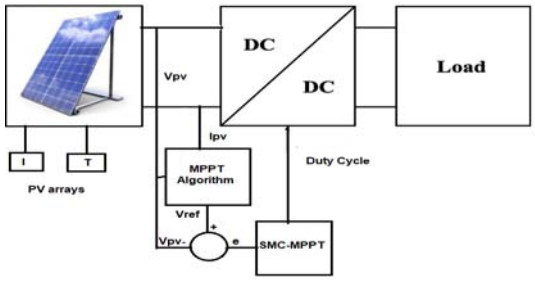

Fig.1. The basic structure photovoltaic system

Table 1. KC200GT Data Sheet under STC Conditions and internal parameters

Number of cells in series of each panel (N_s)	54
Power maximal (P_{max})	200.143 W
Current of short-circuit (I_{sc})	8.21 A
Voltage of circuit open (V_{co})	32.9 V
Current of MPP (I_{mpp})	7.61 A
Voltage of MPP (V_{mpp})	26.3 V
Resistance series (R_s)	0.0036 Ω
Factor ideal (n)	1.4099
Courant inverse de saturation (I_o)	4.0992 e-7 A
Photo current (I_{ph})	8.2100 A

The DC-DC boost converter is installed between PV arrays and load. The values of the parameters of converter as follows:
Resistance (R_h) = 1 Ω, Inductance (L) = 400 µH, Capacitance (C_{out}) = 1200 µF, Capacitance (C_{in}) = 4700 µF, Diode: Resistance (R_{on}) = 0.001 Ω, Direct voltage (V_d) = 0.8 V, damping resistance (R_a) = 500 kΩ, Mosfet: FET Resistance (R_{on}) = 0.1 Ω, Internal diode resistance (R_d) = 0.01 Ω.

The last component in each electrical circuit is the load, we used Resistance R=350 Ω.

PV Cell

Solar cells are used to convert solar energy directly into electrical power. The PV module is made a group of cells which can be connected on series or parallel. The photovoltaic cells analogous circuit is explain in [13, 14]. A

current generator and a diode connect to series and parallel resistors. The equivalent of a single non- ideal solar cell is shown Figure 2. The mathematical equations (1 to 6) define the output current of a single cell.

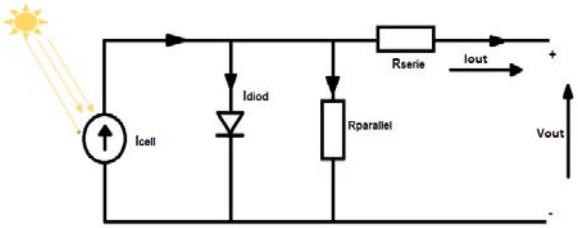

Fig.2. The equivalent circuit model of PV cell.

(1) $$I_{cell} = I_{out} - I_{diod} - I_{parallel}$$

(2) $$I_{diod} = I_0\left[e^{\left(\frac{V_{out}+I_{out}.R_{serie}}{V_{th}}\right)}-1\right]$$

(3) $$I_{out}=I_{Cell}-I_0\left[e^{\left(\frac{V_{out}+I_{out}.R_{serie}}{V_{th}}\right)}-1\right]-\frac{V_{out}+I_{out}.R_{serie}}{R_{parallel}}$$

(4) $$V_{diod} = V_{out} + I_{out}.R_{serie}$$

(5) $$V_{th} = \frac{k.T}{q}$$

(6) $$V_{parallel} = \frac{V_{out} + I_{out}.R_{serie}}{R_{parallel}}$$

I_{out} and V_{out} are cell output current and voltage; I_o is the cell reverse saturation current; I_{cell} is the light-generated current. R_{serie} and $R_{parallel}$ are series and shunt resistances; q is electronic charge;K is Boltzmann's constant; T is cell temperature in K.

DC/DC boost converter

The boost converter is also defined as the step-up converter [15]. It is generally used in the conversion of a low input voltage to a high output voltage[16]. It consists of DC input voltage source V_{PV}, an inductor L, a switch K, a diode, and two capacitors C_{in} and C_{out}. Figure 7 shows the electrical diagram of the proposed boost converter.

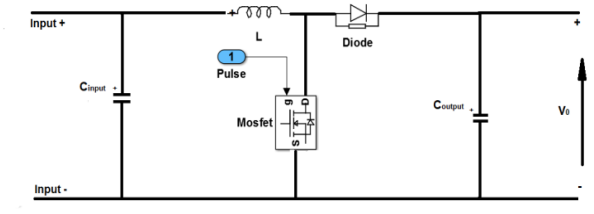

Fig.3. The electrical diagram of the boost converter

The relationship between the input voltage V_{PV} and output V_{out} of the converter is given by the equation (7):

(7) $$V_{out} = \frac{V_{PV}}{D-1}$$

Equations (8) and (9) respectively give the expression of the capacitance and the inductance filter:

(8) $$C = \frac{D.V_a}{f_s.R.\Delta V}$$

(9) $$L = \frac{D.V_a}{f_s.\Delta I}$$

In these relations, D is cycle rapport, f_s is frequency of the Mosfet, ΔV is voltage limit tolerable, ΔI is tolerable current limit and R is load resistance.

In this simulation, we use *fs* = 1000 kHz, ΔV / V = 5% and ΔI / I = 30%. The voltage converter offered has two capacities, Cin and Cout, which have the respective role of reducing the ripple of input and output. For this study, the Mosfet frequency is 1 kHz.

The load

The load is considered constant resistance (R=350 ohms).

MPPT of a stand-alone system (SAS)

Incremental conductance (IC) method

This technique is created to beat the control of P &O MPPT techniques[17]. The IC can determine the MPPT reached and stop perturbing the operating point.

The instantaneous and Incremental conductance of PV arrays utilized to track the MPP at which the maximum power can be tied below as an equation;

(10) $$\frac{I}{V} = \frac{dI}{dV}$$

where dI/dV is the incremental conductance and I/V is the instantaneous conductance.

To get the full control point, must be the power shift and the voltage level ratio are going to zero, according to the derivative rule,

(11) $$\frac{dP}{dV} = \frac{d(V.I)}{dV} = V\frac{dI}{dV} + I$$

At MPP "dP/dV=0" therefore, the instantaneous and incremental conductance becomes opposite and equal as given in (10).

If dP/dV=0 (PV voltage is equal to the MPP) duty cycle should be decreased. If dP/dV < 0 (PV MPP is less than the voltage) duty cycle must be decreased. And if dP/dV > 0, this means the MPP voltage is higher than the PV voltage, and the duty cycle must be augmented[18].

The actual peak power from the PV arrays is determined by IC and P & O. The IC technique is more accurate than P&O technique. In addition, the IC Method shows the exact value of atmospheric change [17].

SMC MPPT technique

It is the theory of structure systems variable (SSV) that allows the task to be accomplished. This control gives stability in results, even with large variations in power or load, and good dynamic, which appeared in the Soviet Union in the 1950 [19][20].

The derivative of power is equal to zero as shown in equation (20) [21]. In the present document, the sliding surface is taken based on equation (12):

(12) $$S = dP$$

The relation expressed the control signal as follows:

(13) $$D = D_{eq} + D_n$$

where U_n is the switching control and Ueq is the equivalent control. U_{eq} found from the steady condition and given as below:

If U=Ueq⇔S=0 & Ṡ=0 the derivative of the sliding surface is:

(14) $$\dot{S} = \frac{d}{dt}[dP] = \frac{d}{dt}[d(V.I)]$$

(15) $$\dot{S} = dV.\frac{dI}{dt} + dI.\frac{dV}{dt} = k_1.\frac{dI}{dt} + k_2.\frac{dV}{dt}$$

(16) $$k_1 = dV \;\&\; k_2 = dI$$

The laws of voltage and current in the circuit in two cases (switch off & on) of Figure 3, by applying Kirchhoff's function:

(17) $$\frac{dI}{dt} = \frac{V_{pv}}{L} - \frac{V_{out}}{L}(1-D)$$

(18) $$\frac{dV_{out}}{dt} = \frac{I_L}{C}(1-D)$$

Substituting Eq. (17) & (18) into Eq. (15) results as:

(19) $$\dot{S} = k_1\left[\frac{V_{pv}}{L} - \frac{V_{out}}{L}(1-D)\right] + k_2\left[\frac{I_L}{C}(1-D)\right]$$

By imposing this is conditions S=0 & Ṡ=0 we get:

(20) $$\dot{S}=0 \rightarrow k_1\left[\frac{V_{pv}}{L} - \frac{V_{out}}{L}(1-D)\right] + k_2\left[\frac{I_L}{C}(1-D)\right] = 0$$

According to Eq. (7), the control input is taken as:

(21) $$D_{eq(t)} = 1 - \frac{V_{pv}}{V_{out}}$$

The trajectory of the sliding surface is so essential, that the U_n is selected for the stability criterion (Ṡ.S <0).

(22) $$D_{n(t)} = \frac{V_{pv}}{V_{out}} - B$$

Where B is calculated according to Lyapunov's stability criteria and considered as a control signal.
Substituting Eq. (21) and Eq. (22) into Eq. (23) as follows:

(23) $$D_t = 1 - B$$

The Lyapunov function adopted to explain the stability

(24) $$P = \frac{1}{2}S^2 Then : \dot{P} = S\dot{S}$$

Replace Eq. (19) and Eq. (24) with Eq. (25), which shows the following result:

(25) $$\dot{P} = (k_1\left[\frac{V_{pv}}{L} + \frac{V_{out}}{L}B\right] - k_2\left[\frac{I_L}{C}B\right])S$$

(26) $$\dot{P} = (B[\frac{V_{out}}{L}.k_1 - \frac{I_L}{C}.K_2] + \frac{V_{pv}}{L}.k_1)S$$

The convergence result is given below.

$$\begin{cases} if S<0 \Rightarrow B < \dfrac{V_{pv}.k_1.C}{V_{out}.k_1.C - I_L.k_2.L} \\ if S>0 \Rightarrow B > \dfrac{V_{pv}.k_1.C}{V_{out}.k_1.C - I_L.k_2.L} \\ if S=0 \Rightarrow B = \dfrac{V_{pv}.k_1.C}{V_{out}.k_1.C - I_L.k_2.L} \end{cases}$$

Simulation Results and Discussion

The simulation is implementing used three PV module KC200GT in series and tow parallel connection, which are monitored by INC and SMC controllers. The controllers are monitoring the performance of the stand-alone system which has been designed and simulated in Matlab / Sim Power.

The irradiation and the temperature used are variable as shown in figures (4&5) and the load is considered constant R = 350Ω.

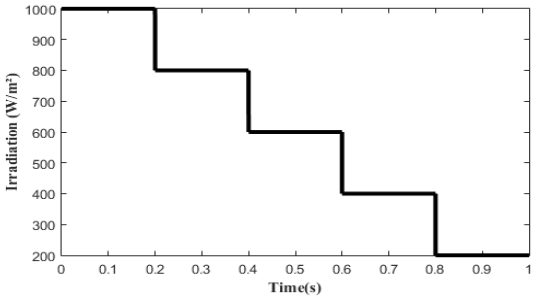

Fig.4. The variation of irradiation

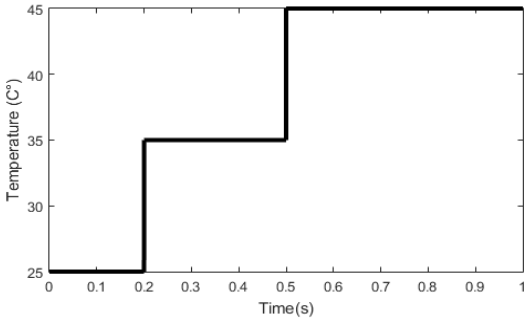

Fig.5. Variation of Temperature

The irradiations were varies as chosen in figure (4) and the temperature was set at T =25°, where the curves show the results in Figures (6&7):

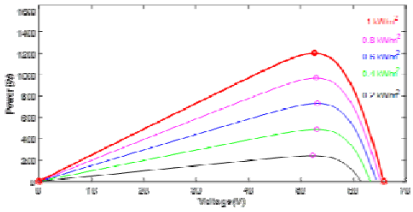

Fig.6. The Voltage-Power characteristic with different irradiation

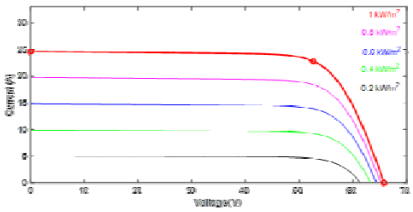

Fig.7. The Current-Voltage characteristic with different irradiations

The temperatures varied as chosen in figure (5) and the irradiation was set at 1000 W/m^2, where the curves show the results in Figures (8&9):

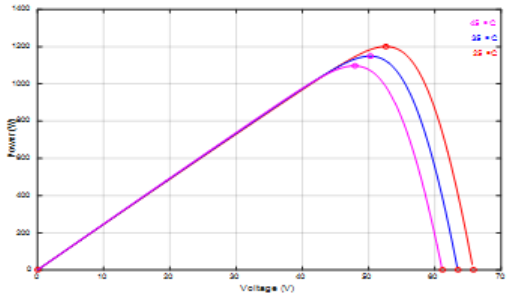

Fig.8. The Voltage-Power characteristic with different temperatures

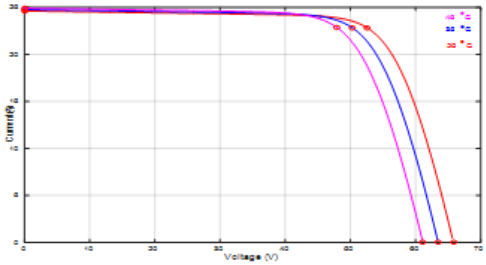

Fig.9. The Voltage-Current characteristic with different temperatures

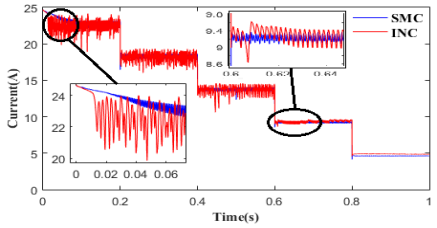

Fig.10. Output Current of PV KC200GT arrays

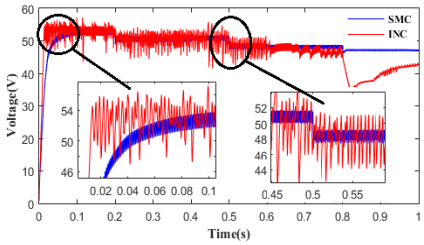

Fig.11. The output voltage of PV KC200GT arrays

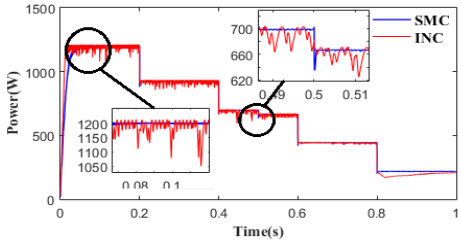

Fig.12. Power of PV KC200GT arrays

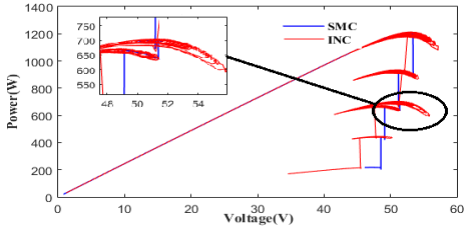

Fig.13. Dynamic MPPT of PV KC200GT arrays

As changing quickly of atmospheric conditions, the simulation results obtained on the MPP for the sliding mode control and INC. The sliding mode control (SMC) give good response in Figures (11) and show the ability to stabilize the voltage in adjacent the voltage required. The INC is reaching the required voltage with chattering and after 0.8 second, the voltage drops below requirement.

Figure (10) shows the output current when the temperature increase and the irradiance decrease automatically. The current drops in two controllers. The SMC gives a good response and without high perturbation than INC controller.

The objective of this paper is obtaining the maximum power from PV arrays. In Figure (12), SMC controller performs accurate in tracking and stability when the is a changing in climatic condition. While INC controller have a high perturbation during climatic changing and around MPP. Also INC controller can't keep the requirement of load during low irradiation or high temperature condition.

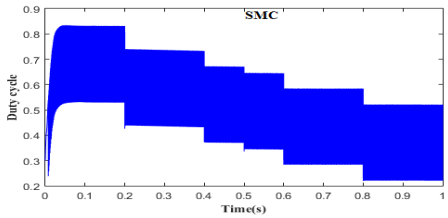

Fig.14. The duty cycle of PV arrays by sliding mode control

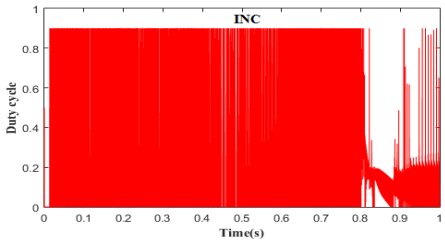

Fig.15. The duty cycle of PV by incremental conductance

The deferent is so clearly in figures (14, 15), the optimum duty cycle of SMC shows the same reaction on each step, and the trucking graph proposed in figure (4), a robust and fast response.

The duty cycle of INC has a perturbation not stable, not reliable and loss the control after 0.8 s.

Conclusion

According to the results of the simulation ,the sliding mode control provides a better design in stand-alone PV arrays system. And its performs significantly better under high variation of environmental condition comparative to conventional INC-MPPT, in terms of overshoot, ripple, speed and accuracy. Moreover, the SMC-MPPT effectively enhances the dynamic responsiveness. The precise tracking of the proposed technique is also shown in the simulation.

Authors:

Ph.D student: Beddi Abdelraouf Email: abdelraouf.beddi@univ-tebessa.dz , Laboratory of Environment Institute of Mines, Department of Science Technology, University Larbi Tébessi-Tebessa, Algeria.

Dr: Hicham Serhoud Email: serhoud-hicham@univ-eloued.dz , Faculty of Technology, Departement of Electrical Engineering, University of El-Oued, El-oued, Algeria.

Pr: Hebbir Nacer Email: habnacer@gmail.com; Laboratory of Materials and Structure of Electromechanical Systems and their Reliability (LMSSEF),Faculty of Exact Sciences, Natural and Life Sciences, Departement of Material Sciences, University of Larbi Ben M'hidi, Oum El Bouaghi, Algeria.

The correspondence address is:abdelraouf.beddi@univ-tebessa.dz

REFERENCES

[1] M. K. H. Rabaia *et al.*, "Environmental impacts of solar energy systems: A review," *Sci. Total Environ.*, vol. 754, p. 141989, 2021.

[2] https://www.nrel.gov/pv/assets/pdfs/best-research-cell-efficiencies-rev220126b.pdf.

[3] A. Hebib, T. Allaoui, A. Chaker, B. Belabbas, and M. Denai, "A comparative study of classical and advanced MPPT control algorithms for photovoltaic systems," *Przegląd Elektrotechniczny*, vol. 96, 2020.

[4] R. I. Putri, S. Wibowo, and M. Rifa'i, "Maximum power point tracking for photovoltaic using incremental conductance method," *Energy Procedia*, vol. 68, pp. 22–30, 2015.
[5] M. I. Bahari, P. Tarassodi, Y. M. Naeini, A. K. Khalilabad, and P. Shirazi, "Modeling and simulation of hill climbing MPPT algorithm for photovoltaic application," in *2016 International Symposium on Power Electronics, Electrical Drives, Automation and Motion (SPEEDAM)*, 2016, pp. 1041–1044.
[6] K. Guo, L. Cui, M. Mao, L. Zhou, and Q. Zhang, "An improved gray wolf optimizer MPPT algorithm for PV system with BFBIC converter under partial shading," *Ieee Access*, vol. 8, pp. 103476–103490, 2020.
[7] A. Badis, M. N. Mansouri, and M. H. Boujmil, "A genetic algorithm optimized MPPT controller for a PV system with DC-DC boost converter," in *2017 International Conference on Engineering & MIS (ICEMIS)*, 2017, pp. 1–6.
[8] S. D. Al-Majidi, M. F. Abbod, and H. S. Al-Raweshidy, "Design of an intelligent MPPT based on ANN using a real photovoltaic system data," in *2019 54th International Universities Power Engineering Conference (UPEC)*, 2019, pp. 1–6.
[9] N. H. Saad, A. A. El-Sattar, and A. E.-A. M. Mansour, "Improved particle swarm optimization for photovoltaic system connected to the grid with low voltage ride through capability," *Renew. Energy*, vol. 85, pp. 181–194, 2016.
[10] D. Pathak, G. Sagar, and P. Gaur, "An application of intelligent non-linear discrete-PID controller for MPPT of PV system," *Procedia Comput. Sci.*, vol. 167, pp. 1574–1583, 2020.
[11] B. Laxman, A. Annamraju, and N. V. Srikanth, "A grey wolf optimized fuzzy logic based MPPT for shaded solar photovoltaic systems in microgrids," *Int. J. Hydrogen Energy*, vol. 46, no. 18, pp. 10653–10665, 2021.
[12] R. Pradhan and A. Panda, "Performance evaluation of a MPPT controller with model predictive control for a photovoltaic system," *Int. J. Electron.*, vol. 107, no. 10, pp. 1543–1558, 2020.
[13] F. Valenciaga and F. A. Inthamoussou, "A novel PV-MPPT method based on a second order sliding mode gradient observer," *Energy Convers. Manag.*, vol. 176, pp. 422–430, Nov. 2018, doi: 10.1016/J.ENCONMAN.2018.09.018.
[14] H. N. Kadeval and V. K. Patel, "Mathematical modelling for solar cell, panel and array for photovoltaic system," *J. Appl. Nat. Sci.*, vol. 13, no. 3, pp. 937–943, 2021.
[15] D. Toumi *et al.*, "Optimal design and analysis of DC–DC converter with maximum power controller for stand-alone PV system," *Energy Reports*, vol. 7, pp. 4951–4960, 2021.
[16] R. Palanisamy, K. Vijayakumar, V. Venkatachalam, R. M. Narayanan, D. Saravanakumar, and K. Saravanan, "Simulation of various DC-DC converters for photovoltaic system," *Int. J. Electr. Comput. Eng.*, vol. 9, no. 2, p. 917, 2019.
[17] A. Raj, S. R. Arya, and J. Gupta, "Solar PV array-based DC–DC converter with MPPT for low power applications," *Renew. Energy Focus*, vol. 34, pp. 109–119, 2020.
[18] L. Shang, H. Guo, and W. Zhu, "An improved MPPT control strategy based on incremental conductance algorithm," *Prot. Control Mod. Power Syst.*, vol. 5, no. 1, pp. 1–8, 2020.
[19] A. T. Azar and Q. Zhu, *Advances and applications in sliding mode control systems*. Springer, 2015.
[20] H. Mekki, D. Boukhetala, and A. T. Azar, "Sliding modes for fault tolerant control," in *Advances and applications in sliding mode control systems*, Springer, 2015, pp. 407–433.
[21] B Tahar, M Djillali, and Halbaoui Khaled "Maximum Power Point Tracking under simplified sliding mode control based DC-DC boost converters," *PRZEGLĄD ELEKTROTECHNICZNY, R. 97 NR 7/2021,pp.60-65.*